Neutral Point Voltage Control Method for Three-Level Diode-Clamped Converter based on Fourth Harmonic Current Injection

Chen Li, Tao Yang, Serhiy Bozhko, Patrick Wheeler
Department of Electrical and Electronic Engineering
University of Nottingham, Nottingham, UK
chen.li@nottingham.ac.uk

***Abstract*—DC-link neutral point voltage balancing for three level neutral point clamped converters has been extensively investigated. Many effective methods have been reported with desirable performances under high power factor conditions. However, most of the reported methods tend to be weakened when the converter operates at lower power factor, and very few methods can function under no-load or light-load condition. This paper proposes an alternative DC-link neutral point voltage control method based on injection of fourth order harmonic current. The proposed method works in full power factor range and no-load condition, where most other methods become less effective. A detailed description of the formulation, control of the method followed by simulation results are presented to confirm the performance of the method.**

Keywords—Neutral-Point-Clamped, Three-level converter

I. INTRODUCTION

The More Electric Aircraft (MEA) notion aims at replacing various pneumatic, hydraulic and mechanical systems on aircrafts with their electrical equivalents, thus increasing energy efficiency and reducing fuel consumption. Aircraft electric starter generator (ESG) system is one of the key technologies within the MEA. Figure. 1 shows a recently emerged ESG configuration for aircraft DC-power system [1][2], where the rotor of a permanent magnet synchronous machine (PMSM) is connected to the shaft of aircraft engine and a three level neutral point clamped (3L-NPC) converter (DC/AC converter) is used as an interface between the aircraft DC power system and the PMSM. During engine start, the converter drives the PMSM to accelerate the engine compressor to ignition speed. However, for most of the time, the converter functions as an active rectifier which extracts energy from the engine shaft and supply various on-board loads via the DC-bus.

Originally proposed for medium voltage applications, the 3L-NPC converter has been receiving more attention in low voltage applications where high efficiency and high fundamental frequency are required [3]. Among commonly-seen multilevel converter topologies such cascaded H-bridges (CHB), flying capacitors (FC) and modular multilevel converter (MMC), the NPC topology is also favoured in transport applications as it requires minimum amount of hardware to generate multiple voltage levels. However, for 3L-NPC converter, one disadvantage is the possible DC-link neutral point voltage imbalance, which leads to output voltage distortion on the AC side and potential capacitor overvoltage on the DC side [4][5].

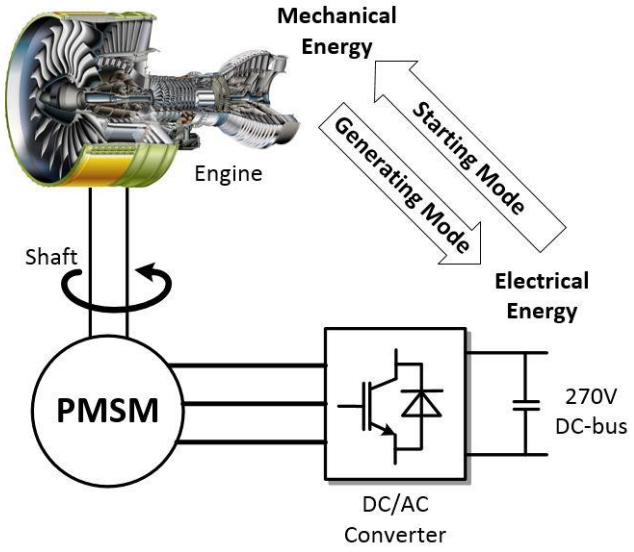

Figure. 1. Illustration of an aircraft electric starter generator system (ESG)

For the continuous DC imbalance, a simple and widely-adopted method is reported in [6]. The method injects common-mode voltage based on a PI controller driven by neutral point voltage imbalance. As the common-mode voltage would not draw current on the AC side, the neutral point voltage can be balanced without impairing current THD. However, this method becomes less effective under lower power factor. For space vector modulations (SVM) [7], a classic neutral point imbalance solution is to play with the redundancy offered by small vectors. As the difference between opposite small vectors is their common-mode voltage, hence the polarities of their neutral point current, manipulation of duty-cycles of redundant small vectors is effectively

manipulation of common-mode voltage. The performance of SVM with small vector manipulation is dependent on modulation index and power factor, where the peak of its balancing capability resides in medium modulation index with unity power factor, and the balancing capability is significantly weakened at high modulation index and low power factor region. For common-mode voltage injection based methods, another solution is reported in [8], where the common-mode voltage required to balance the DC-link neutral point under certain degree of neutral point voltage imbalance is either directly calculated or obtained using a search-optimization approach. The direct calculation method proposed represents a more accurate common-mode voltage injection method in comparison to the previous PI controller based method, but its balancing capability is still limited by modulation index and power factor. For neutral point voltage balancing at low power factor, a six-harmonic voltage injection method is proposed in [9] with desirable performance. The study in [10] pointed out that the balancing capability of the six-harmonic injection method is weakened at high power factor operation, and a hybrid neutral point balancing method is proposed. The proposed hybrid combines the direct-calculation common-mode voltage (pure DC signal) injection method and the six-harmonic injection method, thus offering balancing capability with full power factor range. However, for 3L-NPC converter that operates as an active rectifier under light-load or no-load condition, all above-mentioned methods would become less effective as the magnitude of phase currents is small, or the power flowing between the converter and load is predominantly reactive.

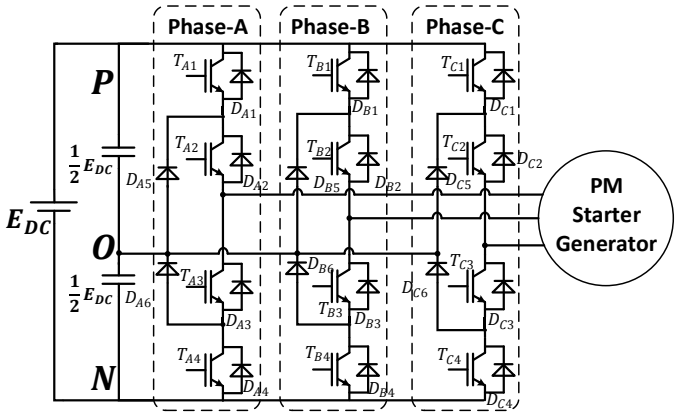

Figure. 2. PMSM driven by a 3L-NPC converter

The 3L-NPC converter also has a self-balancing effect. The study in [11] establishes a mathematical model and proves that self-balancing effect commonly seen in 3L-NPC converters originates from the even-order harmonic currents which are caused by neutral point voltage imbalance. Similar conclusion is also given in [12] without detailed mathematical proof. Consequently, an even-order harmonic current injection is reported in [13]. The proposed method injects negative sequence third harmonic voltage signal in synchronous reference frame, and the injected voltage signal translates into second and fourth order harmonic current on the ac side. The injection is controlled by a simple PI controller driven by the neutral point voltage imbalance detected. The advantage of such method is that the current harmonic injection makes the neutral point balancing capability independent from power factor as well as converter loading condition. However it is also notable that the injection of even-order harmonic current of such low-order would clearly undermine the ac-side current THD. On the other hand, it is also questionable that how much of the injected harmonic currents can be absorbed by the neutral point for balancing purpose, hence the efficiency of balancing.

This paper introduces neutral point balancing method based on even order harmonic current injection. An analysis into possible choices of harmonic currents is presented, which establishes the most efficient choice of injection is the fourth harmonic current. A control structure featuring simplicity is elaborated. The performance of the proposed method is proven with simulation results.

II. Converter Basics and Modulation

As presented in Figure. 2, the 3L-NPC converter used in the ESG systems has three phase legs, each phase leg can connect the corresponding machine winding to the positive point (switching state 'P'), neutral point (switching state 'O') and negative point (switching state 'N') of the DC-link. For each 3L-NPC phase leg, each possible switching states with individual switch states and resultant phase leg pole voltages are detailed in Table. I. Effectively, each 3L-NPC phase leg can be seen as a single pole three throw switch.

Phase leg switching state	Switch status x(a/b/c)				Phase leg pole voltage
	T_{x1}	T_{x2}	T_{x3}	T_{x4}	
P	On	On	Off	Off	$\frac{1}{2}E_{DC}$
O	Off	On	On	Off	0
N	Off	Off	On	On	$-\frac{1}{2}E_{DC}$

Table. I. 3L-NPC converter leg switching states

With each phase leg having three available switching states, the 3L-NPC converter has a total number of 27 available switching states, formulating 27 possible voltage space vectors. As illustrated in Figure. 3, all 27 available voltage space vectors can be converted to coordinates in $\alpha\beta$ frame using Clarke transformation, large vectors are marked with yellow arrows, their magnitudes being $\frac{2}{3}E_{DC}$. Medium vectors are marked with blue arrows, their magnitudes being $\frac{\sqrt{3}}{3}E_{DC}$.

Small vectors are marked with green arrows, their magnitudes being $\frac{1}{3}E_{DC}$. Null vectors are marked with purple arrows, their magnitudes being zero. Among all 27 voltage space vectors, only medium vectors and small vectors connect one of the machine winding to the DC-link neutral point of the 3L-NPC converter.

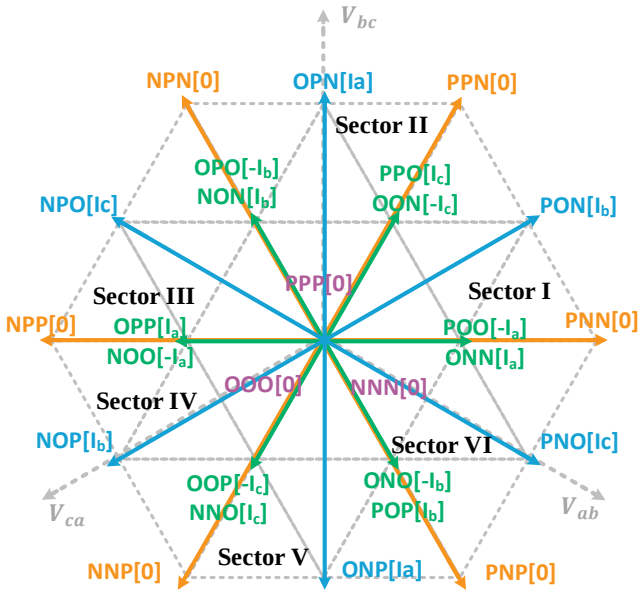

Figure. 3. 3L-NPC voltage space vector diagram

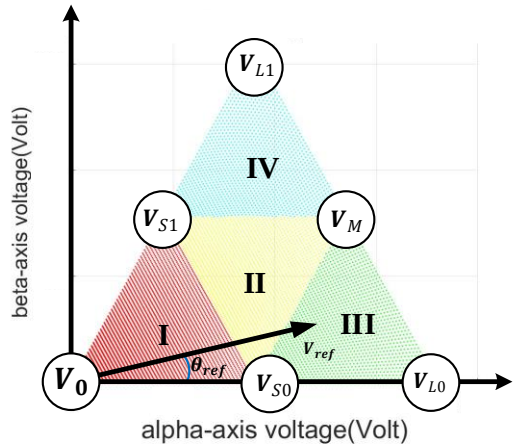

Figure. 4. Conventional 3L-NPC space vector modulation

Take the sector I in the space vector hexagon in Figure. 3 as an example, the conventional space vector modulation technique synthesize the reference vector based on the three most adjacent voltage space vectors. Assume the reference vector falls inside the third region of the sector I as in Figure. 4, the conventional modulation technique will synthesize the reference vector with V_{S0}, V_{L0} and V_M. The duty cycles of each voltage space vector can be calculated based on volt-sec balance principle.

To analyse the neutral point current, this paper assumes the DC-link voltage of the 3L-NPC converter is constant, the upper and lower capacitors are of the same capacitances, and the 3L-NPC converter connects to a balanced load. The positive sequence of three phase reference voltages of the converter can be defined as:

$$\begin{aligned} V_a &= m\cdot\left(2/\sqrt{3}\right)\cdot\cos\theta \\ V_b &= m\cdot\left(2/\sqrt{3}\right)\cdot\cos\left(\theta-2\pi/3\right) \\ V_c &= m\cdot\left(2/\sqrt{3}\right)\cdot\cos\left(\theta+2\pi/3\right) \end{aligned} \tag{1}$$

Where m stands for modulation index and refers to the ratio of the magnitude of the reference voltage vector compared to the maximum voltage in linear modulation area of the space vector hexagon. Fundamental component of the three phase current can be expressed by:

$$\begin{aligned} i_a &= I_s\cdot\cos\left(\theta-\varphi\right) \\ i_b &= I_s\cdot\cos\left(\theta-2\pi/3-\varphi\right) \\ i_c &= I_s\cdot\cos\left(\theta+2\pi/3-\varphi\right) \end{aligned} \tag{2}$$

Where I_s represents the magnitude of the fundamental component of the phase currents, and φ represents the converter power factor angle.

III. Harmonic Selection and Analysis

It is well-established that the neutral point voltage can be affected by the even order harmonics in the phase currents. Possible candidates for even order harmonic injection are the second, the fourth and the eighth harmonic. The eighth order harmonic is excluded as its influence to the neutral point voltage is too weak. Among all available voltage space vectors for a 3L-NPC converter, only small vectors and medium vectors affect neutral point voltage. As the small vector neutral point current is already fully controllable, only the influence from even order harmonic currents to the medium vector neutral point current is analyzed.

$$ITA = \int_0^{Ts} i_{NP}\bullet dt_{Vm} \tag{3}$$

For the ease of analysis, this paper assumes the 3L-NPC is modulated by conventional space vector modulation. The variation of medium vector neutral point current under the influence of even order harmonic currents is referred as current-time-area (ITA), which is obtained by integrating the multiplication of medium vector duty cycle and neutral point current mapped from normalized harmonic current over a fundamental line cycle (Ts). The modulation index is fixed to 0.85 (this fixes the duty cycle) and the displacement angle (denoted as the power factor angle) between the fundamental voltage and selected harmonic current varies.

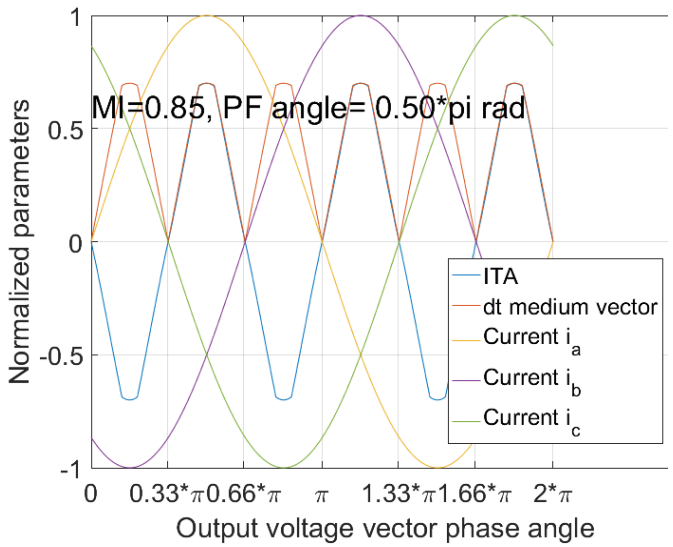

Figure. 5. Illustration of medium vector ITA caused by the fundamental component of three phase currents

To illustrate this, the fundamental current is used as an example in Figure. 5. At a power factor angle of 0.5pi, the normalized ideal three phase currents and the duty cycle of the medium vectors within a fundamental cycle are presented. It's worth noting that the medium vector ITA is obtained by integrating the multiplication of the medium vector duty cycle and the corresponding phase current for the medium vector in a sector ($\pi/3$ radian in Figure. 5).

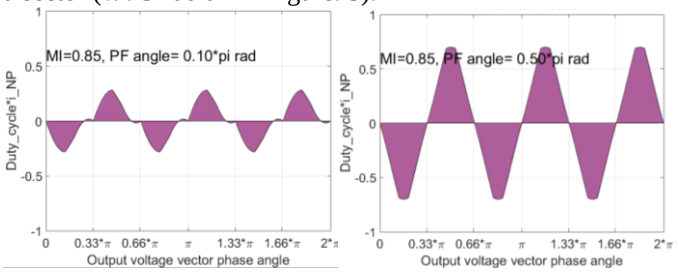

a) b)

Figure. 6. Medium vector ITA caused by the fundamental phase currents under power factor angle of a) 0.1π b) 0.5π

The variation of the medium vector ITA caused by the fundamental phase currents are presented in Figure. 6. It can be seen that at a higher power factor which is 0.1π, the ITA exhibits a ripple three times the fundamental frequency. Whereas at a low power factor of 0.5π, the third harmonic ripple becomes stronger. This phenomenon is in fact the third harmonic ripple which appears at the neutral point of the 3L-NPC converter under high modulation index and low power factor. As seen in Figure. 6, the ideal phase currents of 3L-NPC converters result in an average medium vector ITA of zero, and the overall balancing of the neutral point voltage is not affected despite the third harmonic ripple. However, this is not the case for even order harmonics. Figure. 7 shows the waveforms of the second order harmonic currents and the medium vector duty-cycle. The medium vector ITA caused by the second order harmonic at four different power factor angles are shown in Figure. 8 and Figure. 9 respectively.

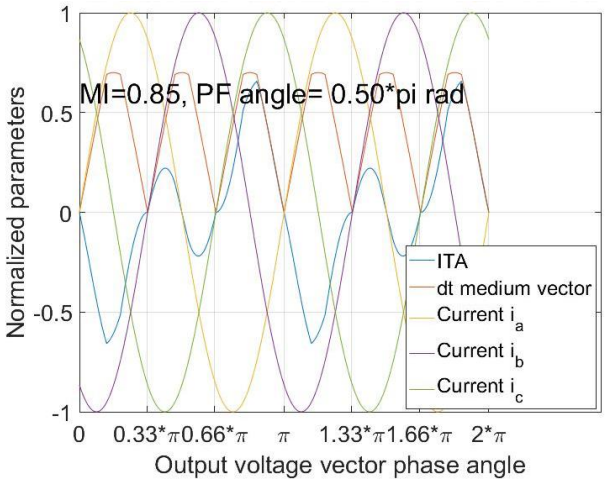

Figure. 7. Illustration of medium vector ITA caused by the second harmonic of three phase currents

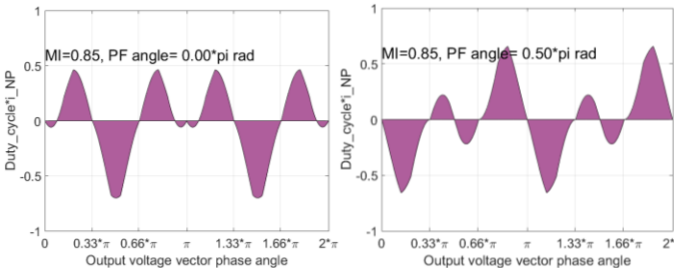

a) b)

Figure. 8. Medium vector ITA caused by the second harmonic phase currents under power factor angle of a) 0 b) 0.5π

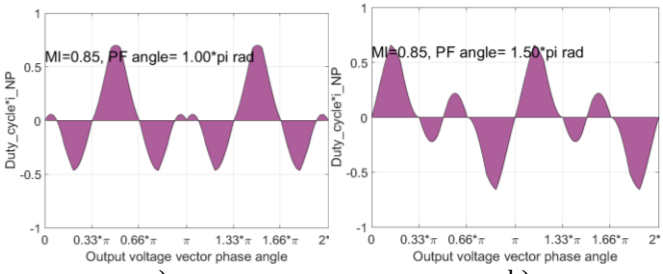

a) b)

Figure. 9. Medium vector ITA caused by the second harmonic phase currents under power factor angle of a) π b) 1.5π

It can be observed from Figure. 8 and Figure. 9 that the total medium vector ITA over a line cycle caused by the second order harmonic under different power factors is not zero under various power factors. This implies when a second order harmonic current component is superimposed onto the fundamental current component, the neutral point voltage of the 3L-NPC converter will drift away from a balanced state. However, it can also be seen from Figure. 8 and Figure. 9 that the medium vector ITA induced by the second order harmonic current results in both charging and discharging of the neutral point regardless of power factors. Therefore, achieving neutral

point voltage control by injecting second order harmonic current may not be efficient.

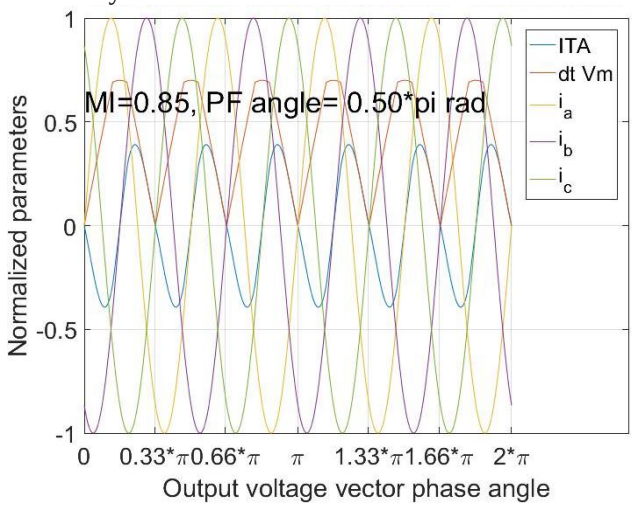

Figure. 10. Illustration of medium vector ITA caused by the fourth harmonic of three phase currents

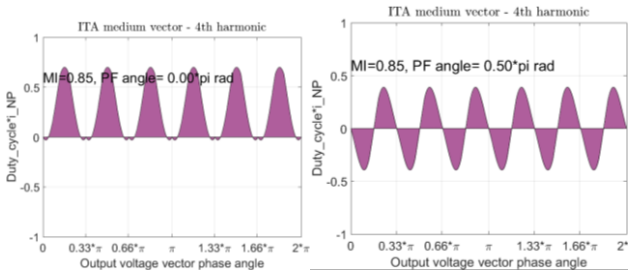

a) b)

Figure. 11. Medium vector ITA caused by the fourth harmonic phase currents under power factor angle of a) 0 b) 0.5π

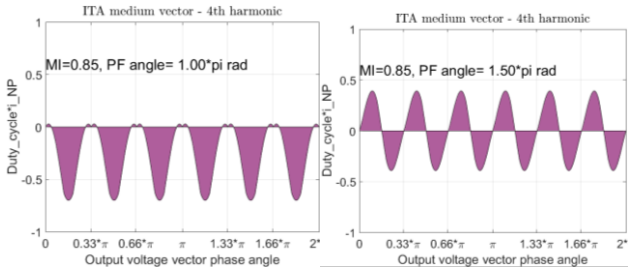

a) b)

Figure. 12. Medium vector ITA caused by the fourth harmonic phase currents under power factor angle of a) π b) 1.5π

The same analysis is also done for the fourth harmonic current. The results are presented in Figure. 10, Figure. 11 and Figure. 12. It can be seen from Figure. 11a) and Figure. 12a) that when the fourth harmonic is injected at power factor of 0 and π, the resultant medium vector ITA can almost be exclusively charging and discharging the DC-link neutral point of the 3L-NPC converter. This implies superimposing a fourth harmonic current at correct phase angle can efficiently achieve the neutral point voltage balancing.

IV. Control Structure

As shown in Figure. 13, the injection of the fourth harmonic current is done by superimposing an additional fourth harmonic reference voltage signal onto the reference voltage generated by the current control loop. The control structure of the ESG system presented in Figure. 13 contains five blocks. The fundamental current loop block takes the synchronous reference frame current references and generates reference voltages for the modulation block. The flux weakening block is activated when the ESG machine is rotating beyond its base speed, this block generates negative d-axis current reference to the current loop to make sure the back-emf of the ESG machine does not exceed available DC-link voltage. When the ESG is in starting mode, the starting block generates q-axis current reference for the current loop to accelerate the engine shaft. In generating mode, a droop controller compare the measured DC-link voltage and generate q-axis current reference for the current loop.

For the fourth harmonic current injection, a simple injection mechanism is devised. The continuous neutral point voltage imbalance is obtained by measuring the DC-link capacitor voltages and applying a low pass filtering afterwards. The voltage imbalance is converted into a reference voltage in the synchronous reference frame of the fourth harmonic voltage. A feedforward angle is calculated based on the ratio between the machine phase resistance and reactance. With the feedforward angle, the fourth harmonic reference voltage is then converted into the ab-frame and is superimposed onto the reference voltages generated by the current loop.

Further to injection, as the injection of the fourth harmonic will slightly increase the THD on the phase currents of the machine, a transition mechanism is implemented to ensure no fourth harmonic current is injected when neutral point voltage is in a balanced condition. With the transition mechanism, the injection of the fourth harmonic reference voltage will be enabled once a continuous neutral point voltage imbalance is detected, and fourth harmonic currents will appear on the ac side and balance the neutral point voltage.

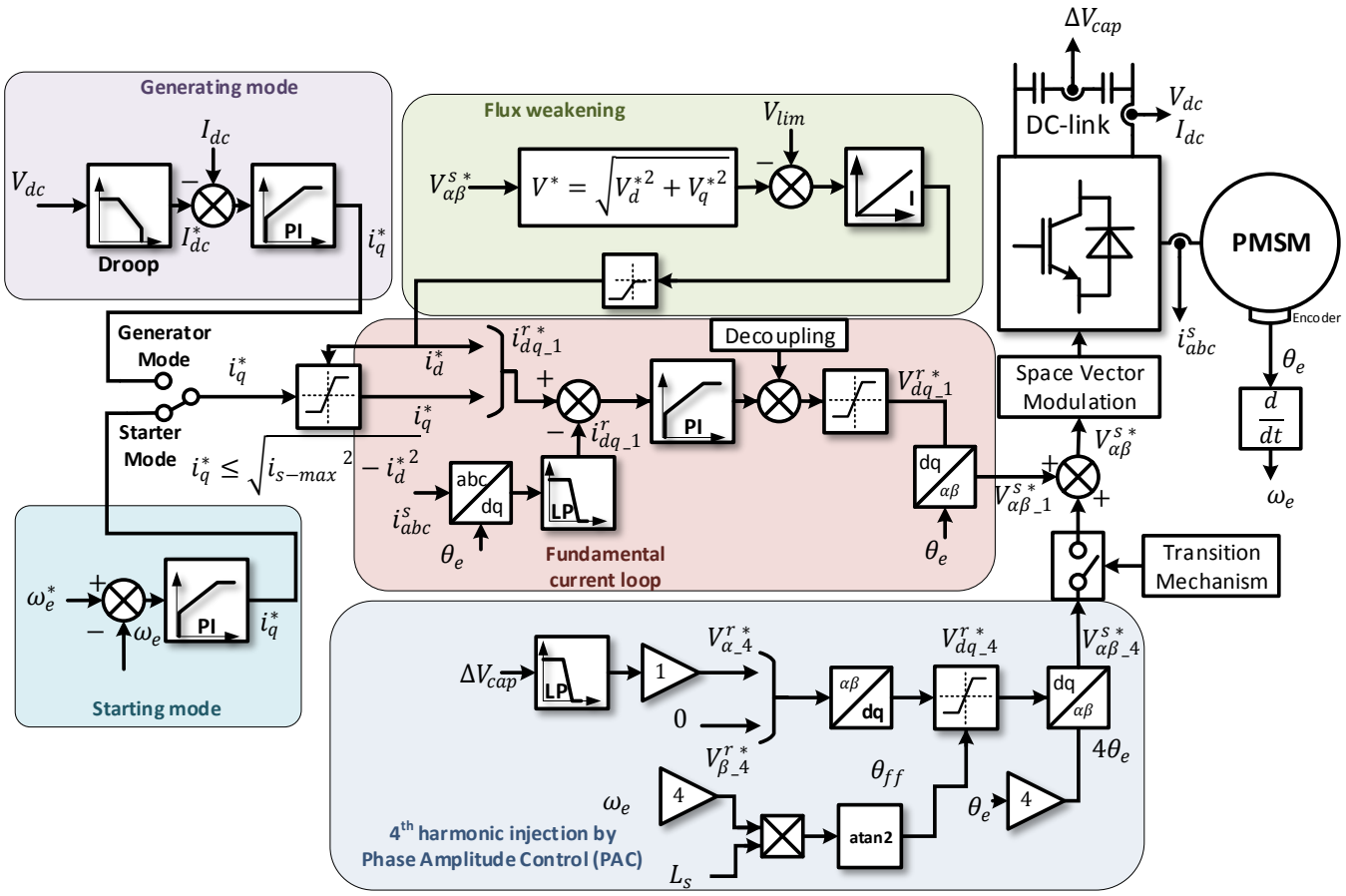

Figure. 13. Proposed control structure for ESG system

V. SIMULATIONS

Simulation results for the proposed 4th harmonic current injection method is obtained with an ESG model implemented in Matlab/Simulink environment. The 3L-NPC converter is supplied by a 270V dc-link, a pair of 600uF capacitors selected. The PMSM driven by the 3L-NPC has pole number of 6, phase resistance of 1.1e-3 Ohm, phase inductance of 99e-6 Henry and PM flux of 0.0364 Vs/rad. At 20krpm of speed, the ESG is in generating mode with no-load, the modulation index is high as deep flux-weakening is required.

A 5Ohm power resistor is connected between DC-link neutral point and ground to induce a voltage imbalance, the injection is enabled at 0.02s, it can be seen that the voltage imbalance is quickly neutralized, thus proving the capability of the proposed method.

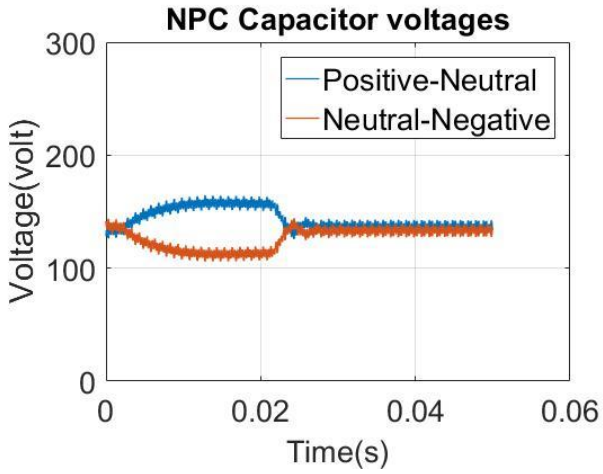

a)

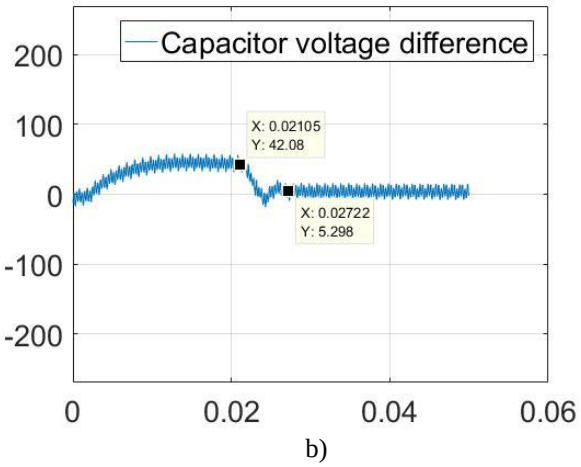

b)

Figure. 14. Simulated DC-link capacitor voltage under imbalance with injection enabled at 0.02s

VI. Conclusion

This paper introduces a neutral point balancing method for 3L-NPC converters based on fourth harmonic current injection, the reason to select 4th harmonic, control structure for phase-amplitude controlled injection and some simulation results are presented. The proposed fourth harmonic current injection, despite slightly increasing the THD on the ac side, can theoretically balance the neutral point voltage of 3L-NPC converter under any power factor condition as long as the medium vector is applied in the modulation process. The validity of the method is confirmed by simulation results.

VII. Acknowledgment

This project has received funding from the Clean Sky 2 Joint Undertaking under the European Union's Horizon 2020 research and innovation program under agreement No 807081.

VIII. References

[1] S. Bozhko, J. Le Peuvedic, T. Yang, P. Arumugam, A. La Rocca, Z. Xu, M. Rashed, W. Fernando, C. Eastwick, C. Gerada, and P. Wheeler, "Development of Aircraft Electric Starter - Generator Systems with Active Rectification Technologies," vol. 44, no. 0.

[2] C. Li, T. Yang, P. Kulsangcharoen, G. Lo Calzo, S. Bozhko, C. Gerada, and P. Wheeler, "A Modified Neutral-Point Balancing Space Vector Modulation Technique for Three-Level Neutral Point Clamped Converters in High Speed Drives," *IEEE Trans. Ind. Electron.*, pp. 1–1, 2018.

[3] M. Schweizer, T. Friedli, and J. Kolar, "Comparative Evaluation of Advanced 3-phase 3-level Inverter/Converter Topologies against 2-level Systems," *IEEE Trans. Ind. Electron.*, vol. 60, no. 12, pp. 5515–5527, 2013.

[4] J. Pou, D. Boroyevich, and R. Pindado, "New feedforward space-vector PWM method to obtain balanced AC output voltages in a three-level neutral-point-clamped converter," *IEEE Trans. Ind. Electron.*, vol. 49, no. 5, pp. 1026–1034, 2002.

[5] J. Pou, R. Pindado, D. Boroyevich, and P. Rodríguez, "Evaluation of the low-frequency neutral-point voltage oscillations in the three-level inverter," *IEEE Trans. Ind. Electron.*, vol. 52, no. 6, pp. 1582–1588, 2005.

[6] C. Newton and M. Sumner, "Neutral point control for multi-level inverters: theory, design and\noperational limitations," *IAS '97. Conf. Rec. 1997 IEEE Ind. Appl. Conf. Thirty-Second IAS Annu. Meet.*, vol. 2, pp. 1336–1343, 1997.

[7] N. Celanovic and D. Boroyevich, "A comprehensive study of neutral-point voltage balancing problem in three-level neutral-point-clamped voltage source PWM inverters," *IEEE Trans. Power Electron.*, vol. 15, no. 2, pp. 242–249, Mar. 2000.

[8] C. Wang and Y. Li, "Analysis and calculation of zero-sequence voltage considering neutral-point potential balancing in three-level NPC converters," *IEEE Trans. Ind. Electron.*, vol. 57, no. 7, pp. 2262–2271, 2010.

[9] H. Akagi and T. Hatada, "Voltage Balancing Control for a Three-Level Diode-Clamped Converter in a Medium-Voltage Transformerless Hybrid Active Filter," *IEEE Trans. Power Electron.*, vol. 24, no. 3, pp. 571–579, Mar. 2009.

[10] J. Shen, S. Schroder, B. Duro, and R. Roesner, "A Neutral-Point Balancing Controller for a Three-Level Inverter With Full Power-Factor Range and Low Distortion," *IEEE Trans. Ind. Appl.*, vol. 49, no. 1, pp. 138–148, Jan. 2013.

[11] J. Shen, S. Schröder, R. Rösner, and S. El-Barbari, "A comprehensive study of neutral-point self-balancing effect in neutral-point-clamped three-level inverters," *IEEE Trans. Power Electron.*, vol. 26, no. 11, pp. 3084–3095, 2011.

[12] J. Pou, D. Boroyevich, and R. Pindado, "Effects of Imbalances and Nonlinear Loads on the Voltage Balance of a Neutral-Point-Clamped Inverter," *IEEE Trans. Power Electron.*, vol. 20, no. 1, pp. 123–131, Jan. 2005.

[13] M. Marchesoni, P. Segarich, and E. Soressi, "A new control strategy for neutral-point-clamped active rectifiers," *IEEE Trans. Ind. Electron.*, vol. 52, no. 2, pp. 462–470, 2005.